20. HUMAN INFLUENCE ON THE 2015 EXTREME HIGH TEMPERATURE EVENTS IN WESTERN CHINA

Ying Sun, Lianchun Song, Hong Yin, Xuebin Zhang, Peter Stott, Botao Zhou, and Ting Hu

Human influence has very likely increased the probability of occurrence of the 2015 western China extreme summer temperature events by at least 3-fold and 42-fold for the highest daily maximum and minimum temperatures, respectively.

Introduction. The 2015 summer (June–August) was historically the hottest in western China (west of 105°E), setting new records for the regionally averaged seasonal mean temperature, annual maxima of daily maximum (TXx), and daily minimum (TNx) temperatures. Many stations set new record high temperatures as well. During the period of 12 June–10 August, the daily high temperature above 38°C covered an area of about 753 000 km², with the highest temperature of 47.7°C recorded in Dongkan station (42.83°N, 89.25°E) of Turpan. The long-lasting extreme high temperature events exerted serious impacts on agriculture and other sectors, resulting in severe heat damage for different crops such as corn, wheat, and fruit trees (CMA 2016).

Data and Methods. The observational data were extracted from the national dataset of homogenized daily temperatures for 1958–2015 with 492 stations in western China (see Fig. 20.1a for a map of station locations) available for the analyses. Even though the station density is poor in some areas, the available station observations represent the region reasonably well because extreme warm events are of fairly large spatial scale. These data were quality controlled and homogenized with RHtest (Xu et al. 2013) by the China National Meteorological Information Center. Two indices representing the hottest day and night temperatures in the summer season, TXx and TNx, were first calculated for individual stations. Regional mean values of TXx and TNx are then computed, with

consideration of uneven spatial distribution of the stations, by first averaging available station data within each 5° × 5° grid box and then taking the averages of the available gridbox values within the region. Based on daily data from climate models participating in the Coupled Model Intercomparison Project Phase 5 (CMIP5; Taylor et al. 2012), the simulated TXx and TNx were used to estimate extreme temperature responses to external anthropogenic and natural forcing (ALL), natural forcing only (NAT), and the internal variability of the climate system. Model data are interpolated onto the same 5° × 5° grids. Detailed information about observations, model data, and calculations are provided in the online supplemental material.

To estimate the influence of anthropogenic forcing (ANT) on the extreme events, our method involves three steps. 1) We first conduct a formal detection and attribution analysis for regional mean TXx and TNx values for 1958–2012 using an optimal fingerprinting method (Hegerl et al. 1997; Allen and Stott 2003) as implemented in Ribes et al. (2013). This is done by regressing the observations onto one or more model-simulated responses to external forcings (ALL, ANT, and NAT). We obtain the scaling factors that scale the model-simulated responses to best match the observations. 2) We then multiply the model simulated responses to ALL and NAT with the relevant scaling factors to obtain the ALL and NAT reconstructions. 3) We finally estimate the probability of occurrence for an event as hot as the 2015 summer in the worlds with or without human influence, using a method described in Sun et al. (2014). The world without human influence is represented by adding preindustrial control simulations to the reconstructed 5-year average model responses to NAT forcing in 2007–12. The world with human influence is represented by adding preindustrial control simulations to the reconstructed 5-year average model response to ALL forcing in 2013–17 that was estimated from simulations from
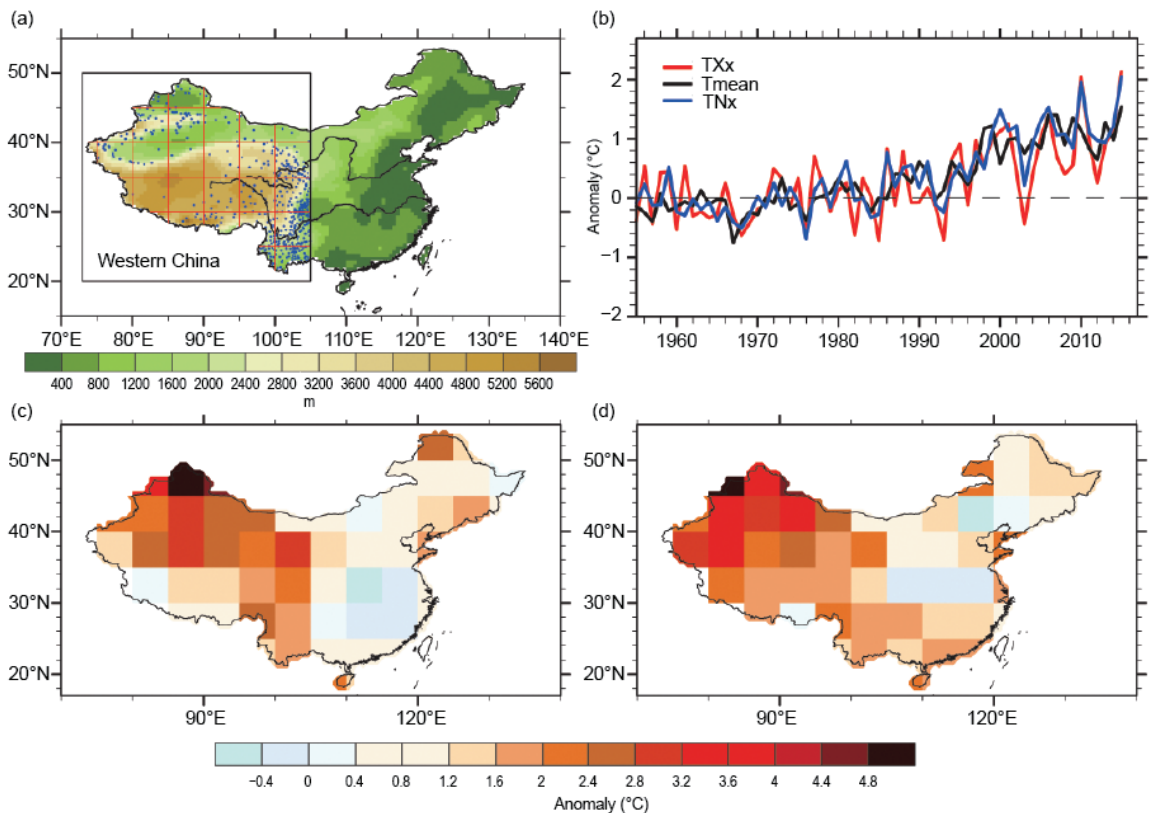
FIG. 20.1. (a) A map of China showing the locations of the observing stations (blue dots) used in the study. The colors show elevation (in meters). (b) Time series of summer mean temperature (black), the maximum daily maximum temperature TXx (red), and the maximum daily minimum temperature TNx (blue) anomalies over western China. (c) Spatial distribution of 2015 summer TXx, and (d) TNx anomalies relative to 1961–90 average (°C).

RCP 4.5 experiments. The percentage of years with temperatures at or above the 2015 summer temperature in the reconstructed series is considered as the probability for that event to occur in the worlds with or without human influence.

The fraction of attributable risk (FAR; Allen 2003; Stott et al. 2004) and its uncertainty range are estimated using a method described in Song et al. (2015). Because the effect of urbanization is not particularly strong in western China, it is not considered in this study.

Results. The regional averages of the 2015 summer (June–August) mean and the TXx and TNx in western China (west of 105°E) were the highest on record beginning in 1958, with 1.54°C, 2.14°C, and 2.06°C above their respective 1961–90 averages (Fig. 20.1b). The long-term changes in the mean and the extreme temperatures are very similar, with the linear trends of 0.28°C (10 yr)⁻¹ for mean temperature, 0.22°C (10 yr)⁻¹ for TXx, and 0.30°C (10 yr)⁻¹ for TNx during 1958–2012, respectively. Warming continued during

the so-called global warming hiatus, consistent with the findings of Seneviratne et al. (2014).

Figures 20.1c,d show the maps of 2015 summer TXx and TNx anomalies in China, respectively. Both the maxima of daily maximum and daily minimum temperatures were very high in western China with positive anomalies almost everywhere in the region. In particular, the anomalies are generally larger than 3°C with the maximum above 5°C in the region north of 35°N.

The 5-year mean time series shows that the evolutions of observed TXx and TNx are consistent with the model-simulated responses to ALL forcing but not with that to NAT forcing (Figs. 20.2a,b). Additionally, the 90% ranges of model-simulated TNx responses to ALL and NAT forcings do not overlap beyond the year 2000. The model-simulated response to NAT forcing shows small positive values near the end of the period, especially for TXx. This might be a reflection of underestimation of volcanic aerosols used in the CMIP5 simulations for the early twenty-first century as suggested by Santer et al. (2014). An implication is
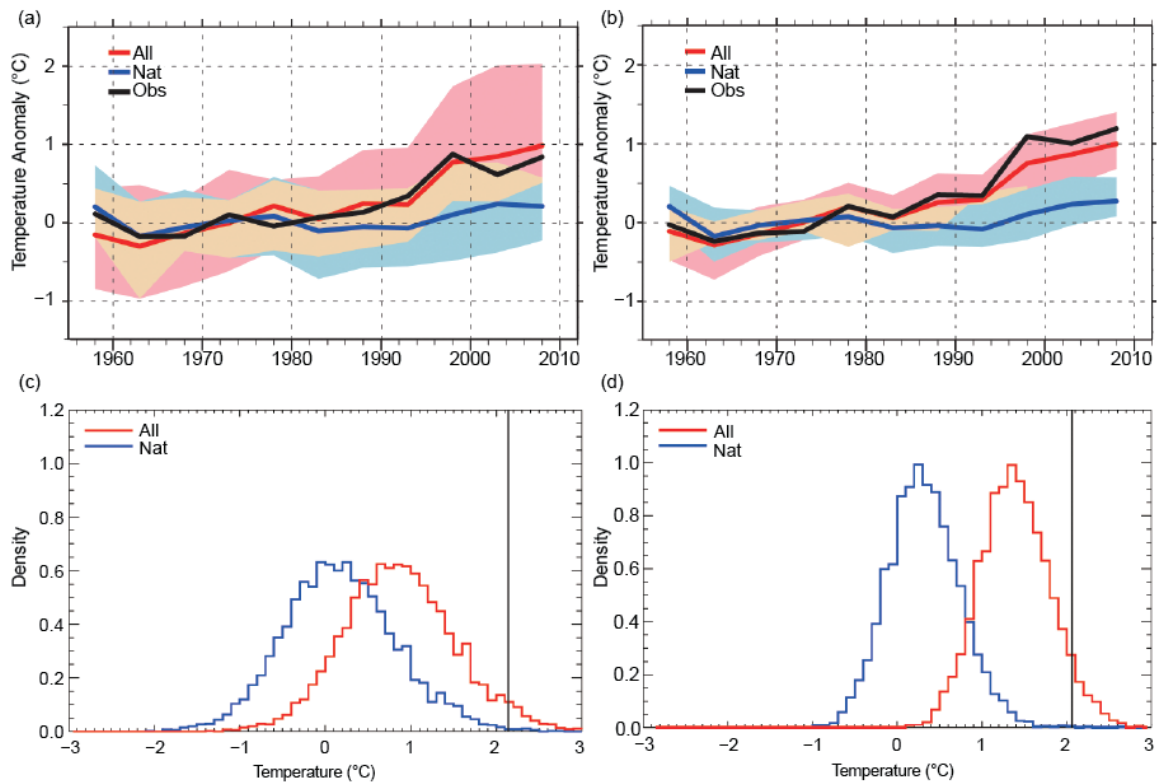
Fig. 20.2. Five-year mean nonoverlapping (a) TXx and (b) TNx anomalies (°C) from observations (black) and simulations of multimodel ensembles. The model ensemble averages are represented by red (ALL) and blue (NAT) lines. The blue and pink shadings show the 5%–95% ranges of the ALL and NAT simulations. (c) Probability histograms for the mean summer TXx and (d) TNx anomalies from the best estimates of NAT (blue) and ALL (red) forcing simulations in comparison with the observed values (OBS, vertical black line) in 2015.

that we might have underestimated human influence on the 2015 summer heat.

Our detection and attribution analyses were conducted on nonoverlapping 5-year mean series. We first regress the observations onto ALL and ALL-NAT (ANT) signals separately (one-signal analyses) and then onto ALL and NAT jointly (two-signal analyses). The one-signal analyses show that the ALL and ANT signals can be detected in the extreme temperatures, and there is no evidence to indicate, from residual consistency tests, that the model may have underestimated natural internal variability. The best estimates of scaling factors for ALL are 0.80 (90% confidence level 0.46–1.14) and 1.20 (90% confidence level 1.00–1.41) for TXx and TNx, consistent with earlier findings (e.g., Zwiers et al. 2011; Kim et al. 2015) for that general region yet over a much larger area.

The two-signal detection results indicate that the ANT signal can be separately detected from the NAT signal for both TXx and TNx, and that the NAT signal can be detected in TNx. The scaling factors for ANT and NAT are 0.78 (90% confidence level 0.38–1.18)

and 0.89 (90% confidence level −0.16–1.95) for TXx and 1.21 (90% confidence level 0.96–1.47) and 1.17 (90% confidence level 0.48–1.87) for TNx, indicating the robustness of detectable human influence on the extreme temperatures. The residual consistency test shows that the model-simulated variability for TXx is consistent with the observed internal variability; however, the model-simulated TNx variability is larger than that of observations. These all suggest that the observed warming in the extreme temperatures are mainly attributable to anthropogenic external forcing rather than natural external forcing.

The 2015 summer TXx was 2.14°C higher than the 1961–90 average. The best estimate of temperature response to ALL forcing at the 2015 climate is 0.88°C (with a 90% range of 0.51°C–1.26°C) above the 1961–90 climatology. This suggests that 1.26°C of the TXx anomaly was due to natural internal variability. By calculating the percentage of years with TXx temperature anomalies at or above 2.14°C in the reconstructions with ALL forcing and with the NAT forcing, the hot 2015 TXx would be roughly a

once-in-272-year event (with a 90% range of 143–572 years) in the natural world, and that it became a once-in-28-year event (with a 90% range of 12–94 years) under the climate appropriate for the anthropogenic-forcing-induced world of 2015. The probability of the event occurring has increased by almost 10-fold due to human influence; there is more than a 90% chance for this increase to be at least 3-fold. The FAR (Stott et al. 2004) can thus be estimated as 0.90 (with a 90% range of 0.66–0.96).

The 2015 summer TNx was 2.06°C above its 1961–90 average. The best estimate of temperature response to ALL forcing at the 2015 climate is 1.40°C (with a 90% range 1.17°C–1.65°C) above the 1961–90 climatology. This suggests that 0.66°C of the TNx anomaly was due to natural internal variability. We estimate that the observed extreme warm temperature for 2015 would be a once-in-1430-year event (with a 90% range of 715–2860 years) in the NAT world, and that it became a once-in-16-year event (with a 90% range of 6–41 years) under the climate appropriate for the anthropogenic-forcing-induced world of 2015. The probability of the event occurring has increased by almost 89-fold due to human influence; there is more than 90% chance for this increase to be at least 42-fold. The FAR can thus be estimated as 0.99 (with a 90% range of 0.97–1.00).

Conclusions. We have detected anthropogenic influence on the highest maximum (TXx) and minimum (TNx) temperatures in western China. We found that the record-breaking 2015 summer temperatures are the result of the combination of natural internal variability of the climate system and human emission of greenhouse gases. The natural internal variability may be associated with anomalous anticyclones on a range of time scales, the possible circulation features causing anomalously high temperatures in northwestern China and dryness in the Tibetan Plateau (Chen et al. 2011; Zhu et al. 2011).

We noted a much larger FAR for TNx than for TXx. This may come about for the following reason: the smaller variance in TNx would mean a larger change in the probability for a similar magnitude of temperature increase when compared with TXx. We also noted that the models may have slightly overestimated natural variability in the region. An implication of this is that our calculated changes in probability (and consequently the FAR) may be underestimated.

REFERENCES

Allen, M. R., 2003: Liability for climate change. *Nature*, **421**, 891–892, doi:10.1038/421891a.

——, and P. Stott, 2003: Estimating signal amplitudes in optimal fingerprinting. Part I: Theory. *Climate Dyn.*, **21**, 477–491.

Chen, L., S.-G. Wang, K.-Z. Shang, and D-B. Yang, 2011: Atmospheric circulation anomalies of large-scale extreme high temperature events in Northwest China. *J. Desert Res.*, **31**, 1052–1058.

CMA, 2016: *China Climate Bulletin 2015*. China Meteorological Administration, 50 pp.

Hegerl, G. C., and Coauthors, 1997: Multi-fingerprint detection and attribution of greenhouse-gas and aerosol-forced climate change. *Climate Dyn.*, **13**, 613–634.

Kim, Y.-H., S.-K. Min, X. Zhang, F. Zwiers, L. V. Alexander, M. G. Donat, and Y.-S. Tung, 2015: Attribution of extreme temperature changes during 1951–2010. *Climate Dyn.*, **46**, 1769–1782, doi:10.1007/s00382-015-2674-2.

Ribes, A., S. Planton, and L. Terray, 2013: Application of regularised optimal fingerprinting to attribution. Part I: method, properties and idealised analysis. *Climate Dyn.*, **41**, 2817–2836, doi:10.1007/s00382-013-1735-7.

Santer, B. D., and Coauthors, 2014: Volcanic contribution to decadal changes in tropospheric temperature. *Nat. Geosci.*, **2**, 185–189, doi:10.1038/ngeo2098.

Seneviratne, S. I., M. G. Donat, B. Mueller, L. V. Alexander, 2014: No pause in the increase of hot temperature extremes. *Nat. Climate Change*, **4**, 161–163, doi:10.1038/nclimate2145.

Song, L., Y. Sun, S. Dong, B. Zhou, P. A. Stott, and G. Ren, 2015: Role of anthropogenic forcing in 2014 hot spring in Northern China [in "Explaining Extreme Events of 2014 from a Climate Perspective"]. *Bull. Amer. Meteor. Soc.*, **96 (12)**, S111–S115, doi:10.1175/BAMS-D-15-00111.1.

Stott, P., D. A. Stone, and M. R. Allen, 2004: Human contribution to the European heatwave of 2003. *Nature*, **432**, 610–613.

Sun, Y., X. Zhang, F. W. Zwiers, L. Song, H. Wan, T. Hu, H. Yin, and G. Ren, 2014: Rapid increase in the risk of extreme summer heat in Eastern China. *Nat. Climate Change*, **4**, 1082–1085, doi:10.1038/nclimate2410.

Taylor, K. E., R. J. Stouffer, and G. A. Meehl, 2012: An overview of CMIP5 and the experiment design. *Bull. Amer. Meteor. Soc.*, **93**, 485–498, doi:10.1175/BAMS-D-11-00094.1.

Xu, W.-H., Q. Li, X. L. Wang, S. Yang, L. Cao, and Y. Feng, 2013: Homogenization of Chinese daily surface air temperatures and analysis of trends in the extreme temperature indices. *J. Geophys. Res. Atmos.*, **118**, 9708–9720, doi:10.1002/jgrd.50791.

Zhu, X. H., O. Bothe, and K. Fraedrich, 2011: Summer atmospheric bridging between Europe and East Asia: Influences on drought and wetness on the Tibetan Plateau. *Quat. Intl.*, **236**, 151–157, doi:10.1016/j.quaint.2010.06.015.

Zwiers, F. W., X. B. Zhang, and Y. Feng, 2011: Anthropogenic influence on long return period daily temperature extremes at regional scales. *J. Climate*, **24**, 296–307, doi:10.1175/2010JCLI3908.1.